AIP | Journal of Renewable and Sustainable Energy

Experimental demonstration of performance of a vertical axis marine current turbine in a river

Staffan Lundin, Johan Forslund, Anders Goude, Mårten Grabbe, Katarina Yuen, and Mats Leijon

Citation: Journal of Renewable and Sustainable Energy **8**, 064501 (2016); doi: 10.1063/1.4971817
View online: http://dx.doi.org/10.1063/1.4971817
View Table of Contents: http://scitation.aip.org/content/aip/journal/jrse/8/6?ver=pdfcov
Published by the AIP Publishing

Experimental demonstration of performance of a vertical axis marine current turbine in a river

Staffan Lundin,[a] Johan Forslund, Anders Goude, Mårten Grabbe, Katarina Yuen, and Mats Leijon
Division of Electricity, Department of Engineering Sciences, Uppsala University, Box 534, SE-751 21 Uppsala, Sweden

(Received 20 April 2016; accepted 23 November 2016; published online 8 December 2016)

An experimental station for marine current power has been installed in a river. The station comprises a vertical axis turbine with a direct-driven permanent magnet synchronous generator. In measurements of steady-state operation in varying flow conditions, performance comparable to that of turbines designed for significantly higher flow speeds is achieved, demonstrating the viability of electricity generation in low speed (below 1.5 m/s) marine currents. [http://dx.doi.org/10.1063/1.4971817]

The world's oceans contain a vast energy resource. In particular, wave and marine current power are predicted to provide significant amounts of renewable electricity.[1,2] Several marine current power research projects are underway world-wide, commercial as well as academic.[3,4] Much work has been or is being done on scale-model experiments and numerical modeling,[5–8] and investigations have been and are being performed outside the laboratories as well.[9,10]

The water flow speed at a potential marine current power site is an important factor in determining the possible energy yield from the site. While recent resource assessments include sites with flow speeds as low as 1 m/s (Refs. 11 and 12) or even 0.8 m/s,[13] most full-size, real-world marine current power projects are commercial undertakings which typically focus on sites with significantly higher flow speeds.[4] There appears, then, to be a technological gap to fill, so that low-speed sites may be exploited. If the threshold speed—above which exploitation of a site is meaningful—can be lowered, more sites become available as potential marine current power sites and the exploitable resource world-wide increase.

The Division of Electricity at Uppsala University has been involved in ocean energy research for many years, always with a strong experimental component. After initial laboratory investigations,[14] the first full-scale prototype of a wave energy converter was installed offshore in 2006.[15,16] On the marine current side, focus has always been on slow currents. A prototype permanent magnet synchronous generator was completed and tested in the laboratory.[17,18] Based on this and other work,[19,20] work on a full-scale experimental station was commenced. The turbine was deployed in the river Dalälven at Söderfors in 2013.[21]

An illustration of the turbine and generator is shown in Fig. 1. The turbine is 6 m in diameter and has 5 fixed-pitch blades, 3.5 m in length. The hydrofoil profile is NACA0021 with a 0.18 m chord length. The generator is a direct-driven permanent magnet synchronous generator with 112 poles. Rated power is 7.5 kW at 15 rpm in 1.4 m/s water flow. The location is in a regulated river in the constructed outlet channel of a conventional hydro power plant, some 800 m downstream of the draft tube. This ensures a comparatively smooth geometry of the river bed as well as knowledge of current discharge levels through cooperation with the power plant operator. At the site, the river is 7 m deep and the flow speed typically varies from less than 0.5 m/s up to 1.5 m/s. Acoustic Doppler current profilers (ADCP) are permanently installed on

[a]Author to whom correspondence should be addressed. Electronic mail: staffan.lundin@angstrom.uu.se

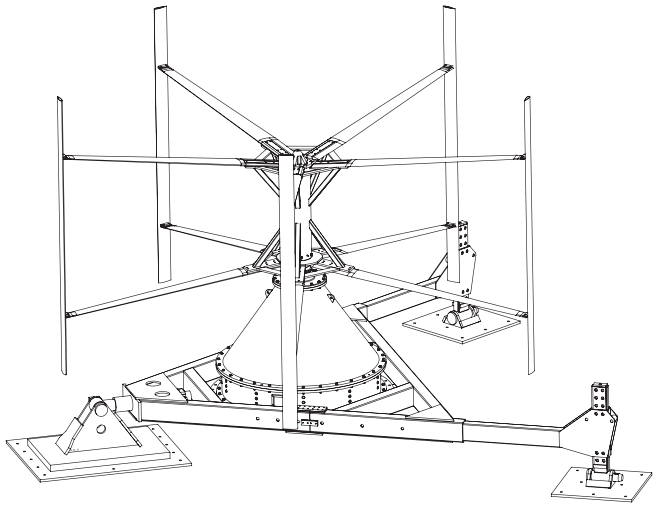

FIG. 1. The turbine and generator housing on their tripod foundation. Illustration by A. Nilsson.

the river bed 2–3 turbine diameters upstream and downstream of the turbine, used for monitoring the flow speed before and after the turbine. A small cabin on shore houses the control system, starting circuit, dump load, and further measurement equipment. Details of the experimental station in general and of the generator in particular, can be found in Refs. 22–24.

To describe the performance of a turbine, the power coefficient C_P is often used. It is defined as

$$C_P = \frac{P_t}{P_0},$$

where P_t is the power captured by the turbine from the water flow and P_0 is the power available in the water flowing through the turbine projected cross-section in undisturbed flow, defined as

$$P_0 = \frac{1}{2}\rho A_t u^3,$$

where ρ is the water mass density, A_t is the turbine cross-sectional area projected in the direction of flow, and u is the water flow speed. Captured power is a function of water speed and turbine angular velocity ω, non-dimensionalised as the tip speed ratio,

$$\lambda = \frac{\omega R}{u},$$

where R is the turbine radius. The power coefficient is usually given as a function of the tip speed ratio, $C_P = C_P(\lambda)$.

To estimate the power coefficient curve of the Söderfors turbine, output power was measured during steady operation with a fixed resistive AC-connected load. By connecting a fixed load, any losses associated with control systems are avoided. On the other hand, water speed is never entirely constant due to turbulence and other variations, so time-averaged values had to be taken.

During measurements, the voltage and current of the dump load were sampled at a rate of 2000 Hz and used for determining the power dissipated in the load. By identifying consecutive zero crossings of the voltage signal, the electrical frequency could be deduced and thence the rotational speed of the generator and turbine. The ADCPs collected readings once in every 3.6 s from 17 measurement bins at 0.25 m intervals. A cubic mean speed was computed over those

measurement bins covering the height of the turbine, and this mean speed value from the upstream instrument was taken as the undisturbed water flow speed.

The turbine was operated with various loads in different water speeds in the interval 1.2–1.4 m/s. Each run lasted for more than 30 min, and time-mean values for rotational speed, water speed, and output power were computed. To obtain the power P_t captured by the turbine, electrical and mechanical power losses were calculated through known parameters of the conversion unit (the efficiency of the generator is discussed in Ref. 24, and frictional losses in bearings and seals were measured before the unit was deployed). The corresponding power coefficients were then computed.

Fig. 2 shows examples of two measurement runs at a nominal flow speed. The load is 2.75 Ω per phase in the first run and 3.35 Ω per phase in the second run. The top subplot in Fig. 2(a) shows the water speed monitored by both the ADCPs (cubic mean speed over the turbine as described above). The downstream instrument shows the wake speed, which goes down when the turbine is operated, slightly more so during the second run when the turbine rotates a little faster. The wake may be expected to be fully developed within approximately 1 min from the turbine start. Rotational speed in rpm is shown in subplot (b) and output power in subplot (c).

The distinct power spike at the beginning of runs is due to the mode the load is connected. There is a short time span (<1 s) during startup when the turbine spins free, after the starting

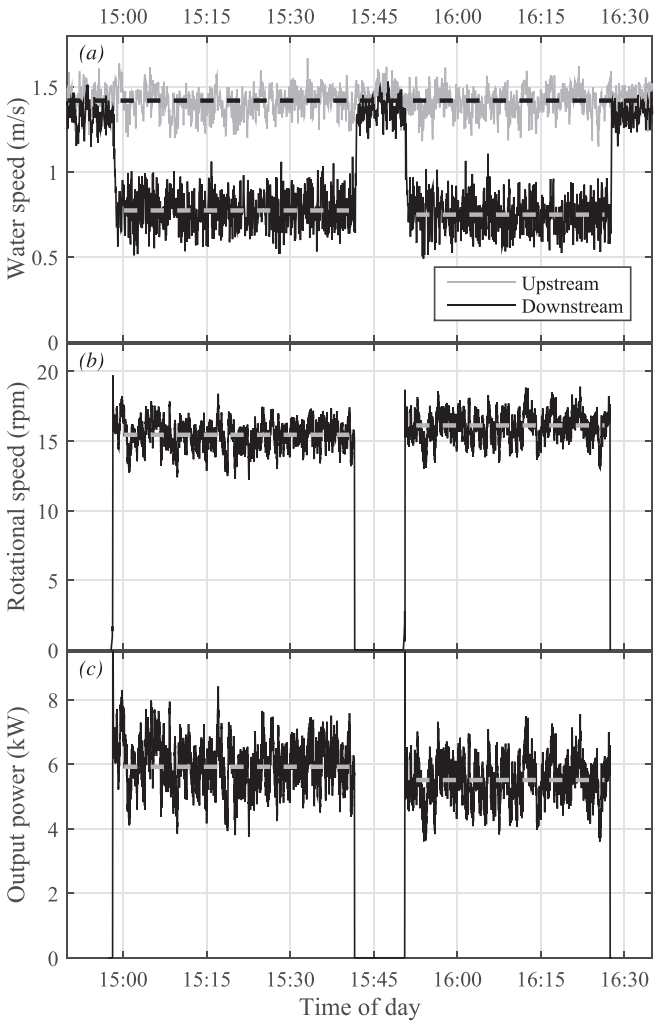

FIG. 2. Example of a measurement sequence taken in water flow speed 1.4 m/s. Dashed lines indicate time-mean values.

circuit is disconnected but before the load is connected. During this time, power captured by the turbine does not leave the rotating system but instead contributes to the rotational energy and thereby the rotational speed. This causes a small spike in a rotational speed at the beginning of runs, most clearly visible in the first run. The extra rotational energy is quickly dissipated in the load once it is connected, in turn causing the very high output power spike, clearly visible for both runs. The mean values (marked in the plot by dashed lines) are calculated beginning 2 min into each run, when any transients have dissipated and a wake has had time to build up downstream of the turbine, and so the spikes will not influence the obtained power coefficients.

The tip speed ratios during the two runs are 3.4 and 3.6, respectively. From Fig. 2, it is clear that a lower resistance in the load (first run) results in a slower rotation of the turbine and also a higher output power. This is due to both runs being at a higher than optimal tip speed ratio. In this region, the power coefficient decreases with increasing rotational speed and tip speed ratio. The power coefficient was 0.26 during the first run and 0.24 during the second run.

Power coefficients from 21 measurement runs are plotted in Fig. 3. According to momentum theory,[25] the driving hydrodynamic torque of a turbine is proportional to flow speed and angular velocity. Hydrodynamic drag causes a torque loss proportional to the angular velocity squared. Power is torque times angular velocity. By these observations and the definitions of power coefficient and tip speed ratio given above, the power coefficient can be estimated as

$$C_P(\lambda) = k_1\lambda^2 - k_2\lambda^3,$$

where k_1 and k_2 are constants associated with hydrodynamic driving torque and hydrodynamic drag. Based on this assumption, Fig. 3 includes a fitted C_P curve where k_1 and k_2 have been determined through least-squares minimization. According to the curve fit, maximum C_P is 0.26 and occurs at the tip speed ratio $\lambda_{\text{opt}} = 3.1$.

To put this C_P figure into perspective, some published results are briefly reviewed. Klaptocz *et al.*[26] performed towing tank tests on a model vertical axis turbine of 0.91 m diameter at 2 m/s flow speed and recorded the power output corresponding to a maximum C_P of approximately 0.2. Alidadi and Calisal[27] numerically modelled a similar turbine and reported a C_P of 0.30 in 1.5 m/s; for comparison, experimental results of $C_P = 0.27$ were also reported. Jing *et al.*[28] made extensive model tests on 0.88 m diameter turbines with varying number of blades with maximum C_P values mainly in the 0.2–0.25 interval. Jing *et al.* also reported C_P values for two tidal current power stations; one rated at 70 kW with design $C_P = 0.26$ in 4.0 m/s flow speed and another rated at 40 kW with $C_P = 0.24$ in 3.0 m/s.

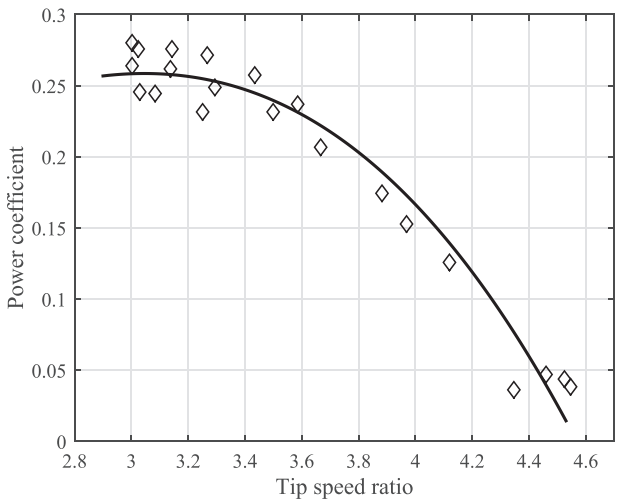

FIG. 3. Power coefficient measurements from flow speeds in the interval 1.2–1.4 m/s, plotted together with a fitted curve. Each sample represents a half-hour average.

Looking again at the results for the Söderfors turbine, it is clear that the efficiency of this turbine operating in flow speeds below 1.5 m/s is essentially the same as that of scale model turbines tested (or simulated) at similar speeds. More interesting, however, is the observation that full-scale turbines designed for considerably higher flow speeds also exhibit power coefficient values in the same region. Thus, the performance of the Söderfors turbine demonstrates the viability of significantly lowering the threshold flow speed for marine current electricity generation.

The work reported was supported by Vattenfall AB, the ÅForsk Foundation, StandUp for Energy, the J. Gust. Richert Memorial Fund, and the Bixia Environmental Fund.

[1]A. S. Bahaj, Renewable Sustainable Energy Rev. **15**, 3399 (2011).
[2]A. Uihlein and D. Magagna, Renewable Sustainable Energy Rev. **58**, 1070 (2016).
[3]A. S. Bahaj, Philos. Trans. R. Soc. A **371**, 20120159 (2013).
[4]Ocean Energy Systems, https://www.ocean-energy-systems.org/library/oes-annual-reports/ for OES annual report, 2014.
[5]M. J. Khan, M. T. Iqbal, and J. E. Quaicoe, IET Renewable Power Gener. **4**, 116 (2010).
[6]P. W. Galloway, L. E. Myers, and A. S. Bahaj, Renewable Energy **63**, 297 (2014).
[7]T. Blackmore, W. M. J. Batten, and A. S. Bahaj, Proc. R. Soc. A **470**, 1 (2014).
[8]Y. Li, N. Karri, and Q. Wang, J. Renewable Sustainable Energy **6**, 1 (2014).
[9]E. Bibeau, S. Kassam, J. Woods, T. Molinski, and C. Bear, J. Ocean Technol. **4**, 71 (2009).
[10]Y. Li, J.-H. Yi, H. Song, Q. Wang, Z. Yang, N. D. Kelley, and K.-S. Lee, Appl. Phys. Lett. **105**, 1 (2014).
[11]L. S. Blunden, A. S. Bahaj, and N. S. Aziz, Renewable Energy **49**, 137 (2013).
[12]S. Bomminayuni, B. Bruder, T. Stoesser, and K. Haas, J. Renewable Sustainable Energy **4**, 063107 (2012).
[13]Z. Defne, K. A. Haas, and H. M. Fritz, Renewable Sustainable Energy Rev. **15**, 2310 (2011).
[14]K. Nilsson, O. Danielsson, and M. Leijon, J. Appl. Phys. **99**, 34505 (2006).
[15]R. Waters, M. Stålberg, O. Danielsson, O. Svensson, S. Gustafsson, E. Strömstedt, M. Eriksson, J. Sundberg, and M. Leijon, Appl. Phys. Lett. **90**, 034105 (2007).
[16]M. Eriksson, R. Waters, O. Svensson, J. Isberg, and M. Leijon, J. Appl. Phys. **102**, 084910 (2007).
[17]K. Thomas, M. Grabbe, K. Yuen, and M. Leijon, Proc. IMechE Part A **222**, 381 (2008).
[18]K. Thomas, M. Grabbe, K. Yuen, and M. Leijon, ISRN Renewable Energy **2012**, 7.
[19]K. Yuen, K. Thomas, M. Grabbe, P. Deglaire, M. Bouquerel, D. Österberg, and M. Leijon, IEEE J. Oceanic Eng. **34**, 24 (2009).
[20]E. Lalander, M. Grabbe, and M. Leijon, J. Renewable Sustainable Energy **5**, 023115 (2013).
[21]S. Lundin, J. Forslund, N. Carpman, M. Grabbe, K. Yuen, S. Apelfröjd, A. Goude, and M. Leijon, in *Proceedings of the 10th European Wave and Tidal Energy Conference, EWTEC13, Aalborg, Denmark* (2013).
[22]M. Grabbe, K. Yuen, A. Goude, E. Lalander, and M. Leijon, Int. J. Hydropower Dams **15**, 112 (2009).
[23]K. Yuen, S. Lundin, M. Grabbe, E. Lalander, A. Goude, and M. Leijon, in *Proceedings of the 9th European Wave and Tidal Energy Conference, EWTEC11, Southampton, UK* (2011), pp. 1–5.
[24]M. Grabbe, K. Yuen, S. Apelfröjd, and M. Leijon, Adv. Mech. Eng. **2013**, 978140.
[25]J. F. Manwell, J. G. McGowan, and A. L. Rogers, *Wind Energy Explained: Theory, Design and Application*, 2nd ed. (Wiley, 2009).
[26]V. R. Klaptocz, G. W. Rawlings, Y. Nabavi, M. Alidadi, Y. Li, and S. M. Calisal, in *Proceedings of the 7th European Wave and Tidal Energy Conference, EWTEC07, Porto, Portugal* (2007).
[27]M. Alidadi and S. Calisal, Comput. Fluids **105**, 76 (2014).
[28]F. Jing, Q. Sheng, and L. Zhang, Ocean Eng. **88**, 228 (2014).